The Cryosphere
Open Access
Discussions

Little Ice Age climate reconstruction from ensemble reanalysis of Alpine glacier fluctuations

M. P. Lüthi

VAW Glaciology, ETH Zürich, 8093 Zürich, Switzerland

Correspondence to: M. P. Lüthi (luethi@vaw.baug.ethz.ch)

Abstract

Mountain glaciers sample a combination of climate parameters – temperature, precipitation and radiation – by their rate of volume accumulation and loss. Flow dynamics acts as transfer function which maps volume changes to a length response of the glacier terminus. Long histories of terminus positions have been assembled for several glaciers in the Alps. Here I analyze terminus position histories from an ensemble of seven glaciers in the Alps with a macroscopic model of glacier dynamics to derive a history of glacier equilibrium line altitude (ELA) for the time span 400–2010 C.E. The resulting climatic reconstruction depends only on records of glacier variations. The reconstructed ELA history is similar to recent reconstructions of Alpine summer temperature and Atlantic Meridional Oscillation (AMO) index. Most reconstructed low-ELA periods coincide with large explosive volcano eruptions, hinting to mass balance reduction by volcanic radiative cooling. The glacier advances during the LIA, and the retreat after 1860 are thus explained by temperature and volcanic cooling alone.

1 Introduction

Proxy-based climate reconstructions are an important source of information on past climate variability and help to assess whether the climate change presently observed is unprecedented in a long-term context (IPCC, 2007). Some of these proxies, notably tree ring data, give a detailed picture of summer temperature variations (e.g. Mann et al., 2009; Büntgen et al., 2006, 2011). Records of glacier length changes (GLCs) provide supplementary independent information, as they are governed by a combination of the same climate variables (summer temperature and radiation, winter precipitation), but are caused by fundamentally different processes.

GLCs have been used in a qualitative manner to confirm climate reconstructions from proxies (Guiot et al., 2010) or compare them with solar forcing reconstructions (e.g. Beer et al., 2009; Nussbaumer et al., 2011). However, such comparisons suffer

from the delayed response of glacier length to climatic or radiative forcing, and are only valid on long time scales.

Mountain glaciers adjust their length to a changing climate at a rate which depends on bedrock geometry and ice thickness distribution. Glaciers can therefore be regarded as climate sensors with geometry-dependent susceptibility and response time. This relationship has been exploited to infer past climate from GLCs with help of glacier models of different complexity. Analytical approximations (Callendar, 1950; Nye, 1963, 1965; Klok and Oerlemans, 2003; Roe and O'Neal, 2009), neural networks (Steiner et al., 2005) and numerical ice flow models (Greuell, 1992; Schmeits and Oerlemans, 1997) have been applied to either single glaciers, an ensemble of glaciers in the same climate region (Oerlemans, 2007), or glaciers distributed around the globe (Hoelzle et al., 2003; Oerlemans, 2005; Leclercq et al., 2011; Leclercq and Oerlemans, 2012).

Several studies showed that numerical models of reduced complexity give volume and length changes that are similar to those calculated with models solving the full equations (e.g. Leysinger-Vieli and Gudmundsson, 2004; Oerlemans, 2011; Lüthi, 2009). A simple model of a mountain glacier describing the delayed response of GLC to volume change is a dynamical system in the variables "length" L and "volume" V derived in Lüthi (2009). Essentially, the glacier behaves as a slightly over-damped harmonic oscillator in one of the macroscopic variables L or V around a steady state (Harrison et al., 2003). The advantage of using a macroscopic model is that no knowledge on the usually complex and insufficiently known glacier bed geometry is required. Instead, two model parameters are determined with an optimization procedure which yields the LV-model with the most similar length response under a given ELA history. Such a dynamically equivalent simple model (DESM) is useful to systematically analyze GLC records (Lüthi and Bauder, 2010), and to infer glacier volume change from GLCs (Lüthi et al., 2010).

Here I use seven very long glacier terminus position records from the Alps to derive glacier equilibrium line altitude (ELA) for the period 400–2010 C.E. The ELA history causing the observed GLCs is determined with an optimization procedure which em-

ploys the macroscopic LV-model for each of the seven glaciers. The resulting glacier ELA variations are completely independent of any other proxy data, and are indicators of summer temperature, winter precipitation and radiation (Vincent et al., 2004; Ohmura et al., 2007; Huss et al., 2009; Thibert et al., 2013). The reconstructed ELA histories are then compared to other proxy-based reconstructions of European summer temperature, total solar irradiance, and volcanic cooling.

2 Data and methods

2.1 Length change data

GLCs have been systematically monitored since about 1860 when most glaciers receded from their last maximum extent of the Little Ice Age cold period (LIA, ca. 1550–1850 C.E.). Older reconstructions are based on photographs, paintings, written records, and the positions of trees destroyed by glacier advance, and dated by dendrochronology or the carbon-14 method. The longest such reconstruction has been assembled for Grosser Aletsch glacier, and similar records exist for the glaciers Gorner, Rhone, Rosenlaui, Unterer Grindelwald, Mer de Glace and Bossons (data sources are listed in Table 1). These historic GLC series have been complemented with recent data from the Swiss Glacier Monitoring Network (Glaciological Reports, 1881–2011) and other sources (Vincent et al., 2005, A. Bauder, personal communication, 2012).

2.2 Macroscopic glacier model

Climatic interpretation of GLC has to take into account the combination of direct and delayed response of the glacier terminus to climate forcing. The direct response is caused by the difference between the rates of ice melt and mass transport to the terminus. Ice melt varies rapidly with changes of temperature and radiation, while mass transport varies slowly due to upstream geometry changes which affect ice flow patterns. A glacier model represents the transfer function from volume change to length

change, and depends on glacier size, bedrock geometry, and surface mass balance distribution.

The simplest such model represents glacier dynamics on a macroscopic level, and results in a dynamical system in the variables "length" L and "volume" V for unit glacier width, referred to as the LV-model (Eq. 40 in Lüthi, 2009)

$$\frac{dV}{dt} = \dot{g}\left(V + ZL - \frac{s}{2}L^2\right), \tag{1a}$$

$$\frac{dL}{dt} = \frac{1}{\tau_a}\left[\left(\frac{V}{a}\right)^{\frac{1}{\mu}} - L\right]. \tag{1b}$$

Here, $\dot{g} = \frac{\partial \dot{b}}{\partial z}$ denotes the vertical gradient of local mass balance rate $\dot{b}$ (in units of velocity, i.e. meter ice equivalent per year and per square meter), and $s = \tan\beta$ is bed slope. Equation (1b) is a relaxation equation for the current glacier length L with time constant τ_a (in years; τ_a should not be confounded with the volume time scale τ_v). The steady state length for the current volume V is determined by a volume-length scaling relation of the form $V = a L^\mu$ with parameters $\mu = 7/5$, and a which depends on $\dot{g}$ and s (Lüthi, 2009, Eq. 21), and which is continually updated for the current glacier length (Lüthi, 2009, Eqs. 37 and 38). The dynamical system (Eq. 1) is driven by a forcing in the term $Z(t) = z_0 - z_{ELA}(t)$, where z_0 is the highest point of the bed and $z_{ELA}(t)$ is the time dependent elevation of the equilibrium line.

2.3 ELA reconstruction

To drive the LV-model and hence calculate glacier response, an ELA history $z_{ELA}(t)$ is prescribed as forcing function, changing the $Z(t) = z_0 - z_{ELA}(t)$ term of Eq. (1a). In the LV-model, local mass balance rate is given as linear function of elevation $\dot{b}(z) = \dot{g}(z - z_{ELA})$ with a constant vertical gradient of local mass balance rate $\dot{g}$. A value of $\dot{g} = 0.008\,\mathrm{yr}^{-1}$ was assumed for this study which is a good average for the central Alps

(e.g. Chen and Funk, 1990; Huss et al., 2008, Table 3); Using $\dot{g} = 0.007\,\mathrm{yr}^{-1}$ changed the results only marginally.

The climate history is represented by constant ELA values within fixed size intervals (10 yr between 0–1200 C.E., 5 yr between 1200–2010 C.E.). These 283 ELA values are unknowns to be determined in an optimization procedure. Additionally, two parameters (slope s and vertical extent $Z_0 = Z(t = 0)$) are sought for each of the seven LV-models representing the seven glaciers. Optimization was performed with two algorithms, leading to very similar results: a Reversible-Jump Markov-Chain-Monte-Carlo (RJ-MCMC) algorithm, and the BOBYQA optimizer (Powell, 2009; Johnson, 2012). The cost function for the optimization is constructed by summing the squares of differences between modeled and measured GLCs. A large penalty was added to the cost in case of violation of one-sided constraints on glacier length (e.g. living trees or terminus moraines). The model runs were initialized with random glacier parameters, and zero (or random) ELA variations.

3 Results

3.1 Reconstructed length changes

Modeled terminus positions calculated with the 20 best-performing ELA histories are compared to the historical records in Fig. 1 (Table 1 for data sources). Modeled terminus positions differ considerably between different model runs during periods without lengths constraints, and are therefore not shown in the figure. During the other periods the agreement with the constraints imposed by the data is good. Life spans and death times of trees (marked with orange horizontal lines and black dots) are mostly achieved. Individual terminus positions since 1600 C.E., when dense data is available, are mostly reconstructed for all glaciers. Root mean square (RMS) differences are smaller than 20 m. Most absolute differences are smaller than 150 m, but are occasionally as high as 300 m. Since the LV-model geometry with a single slope is highly idealized, perfect

agreement between observed and modeled GLCs cannot be expected. Terminus positions are strongly influenced by details of terminus bedrock geometry such as cliffs (steep glaciers Bossons, Mer de Glace, Unterer Grindelwald and Rosenlaui) or terminus areas with strong topographic breaks (Rhone). By using an ensemble of glaciers
5 with different geometries and response characteristics, the dependence of the overall result on such geometric peculiarities is reduced.

The modeled GLCs obtained with the reconstructed ELA histories are robust against 10 % variations of glacier parameters (s, Z_0), 15 % variation in mass balance gradient ($\dot{g}$), and omission of length constraints. During several time periods with small glacier
10 extent no terminus position data is available and modeled terminus positions assume a wide spread of values (around 700, 900, 1000 and 1400–1530 C.E., omitted data in Fig. 1). Consequently, no information on ELA variations during these periods can be extracted, and the modeled terminus positions and reconstructed ELAs can assume a wide variety of values within these periods.
15 The low reconstructed ELAs during the period 1300–1350, only documented from trees killed by the advancing Gorner glacier, lead to large modeled advances of the steep glaciers which exceed the 1850 terminus positions. Indeed, on Rhone glacier several moraine ridges from the early medieval period are documented which could correspond to this reconstructed 1350 maximum position (Zumbühl and Holzhauser,
20 1988). The slowly reacting glaciers Gorner and Grosser Aletsch on the other hand only reach terminus positions that are less advanced than their 1850–1860 maximum.

3.2 Reconstructed ELA history

The reconstructed ELA histories leading to the best agreement between modeled and measured GLCs are shown in Figs. 2–4. Noteworthy are extended periods of low ELA
25 (low summer temperature, reduced incoming radiation, high solid precipitation) which coincide with large and rapid glacier advances. Figure 2 shows high-amplitude ELA oscillations between 1650 and 1830 which correspond to the rapidly varying termi-

nus positions of the steep glaciers (Bossons, Mer de Glace, Unterer Grindelwald and Rosenlaui, Fig. 1).

Periods of high ELA (high summer temperature and radiation, low solid precipitation), corresponding to decreasing or small glacier extents, are mostly missing in the reconstruction before 1600. This is due to the lack of data on shorter glacier extents, traces of which might still be buried under the glaciers. The period with highest ELAs begins after 1980, exceeding the reconstructed values of the preceding 1600 yr. Since present-day glacier geometries have not yet fully adjusted to the climate of the last decades (depending on glacier response time) the reconstructed ELA during the last decades might be considerably higher.

3.3 Comparison with instrumental data

The reconstructed ELA history is compared to instrumental temperature data in Fig. 2. The agreement of summer (JJAS) temperature with the high-Alpine Grand Saint Bernard meteorological station (2500 m a.s.l. Begert et al., 2005) and with the HISTALP CRSM Alpin multi-station reconstruction (Auer et al., 2007) is reassuring. To obtain similar variability of the records, the sensitivity factor between reconstructed ELA and temperature is $f_s = 80$–$100\,\mathrm{m\,K^{-1}}$ (i.e. 80–100 m ELA change per Kelvin temperature change). Similar values are reported in the literature: $97\,\mathrm{m\,K^{-1}}$ (Thibert et al., 2013), $113\,\mathrm{m\,K^{-1}}$ (Oerlemans, 2010), and 60–$70\,\mathrm{m\,K^{-1}}$ (Vincent, 2002).

Comparisons with the HISTALP CRSM NW (Auer et al., 2007) and the Casty et al. (2005) reconstruction of European temperature, reaching back to 1768 and 1500 C.E., are shown in Fig. 2b. The ELA reconstruction shows similar temperature variability after 1820, but is considerably lower before (by 100 m, or 1 K), while the timing of high and low temperature events tends to agree. Such a discrepancy might be caused by a suspected warm bias in the early instrumental data (Frank et al., 2007; Böhm et al., 2010).

3.4 Comparison with proxy records

The reconstructed ELA history was compared to many long climate reconstructions of mid-European temperature from proxy data such as tree rings, lake sediments, ice cores and speleothems. Since glacier mass balance is controlled by a combination of processes, one cannot expect that a single proxy record agrees with the ELA history. In addition, climate variability at high elevation might differ significantly from the low elevations from where most proxy records are recovered.

Figures 3 and 4 compare the reconstructed ELA history to a selection of proxy records that show, at least partially, close similarities. Reconstructions of Atlantic Meridional Oscillation (AMO, Fig. 2c; Mann et al., 2009) and a Northern Hemisphere multi-proxy temperature history (Fig. 3d; Mann et al., 2009) show similar long term behavior, variability and individual cold events after 1200, but are considerably warmer before. The sensitivity factor from ELA to temperature variation is twice that of the instrumental data (Table 2), presumably due to hemispheric averaging of the records. A recent multi-proxy temperature history for Europe (PAGES 2k consortium, 2013, Fig. 4e) is very similar to the ELA reconstruction throughout the considered 1600 yr. It shows most of the early cold events (550, 800, 1100 C.E.) that are absent in other proxy records, but for which marked glacier advances are documented (Fig. 1). Tree-ring based temperature histories of the Alps (Fig. 4f; Büntgen et al., 2006) and central Europe (Fig. 4g; Büntgen et al., 2011) show an overall close agreement with the ELA reconstruction. Tree growth is predominantly a proxy for summer (JJAS) temperature, which coincidentally is the same period which affects glacier melt, and thus glacier mass balance variability (e.g. Huss et al., 2008).

Figure 3b shows that reconstructed ELAs closely follow total solar irradiance (TSI; Steinhilber et al., 2009) during the period 1700–1950, but bear little similarity before 1700. The cooling effect of explosive volcanism can be evaluated with the top panels and gray vertical bars in Figs. 2–4, indicating the Northern Hemisphere stratospheric sulfate load from big volcanic eruptions (Gao et al., 2008, NH, v2). It is noteworthy

that most of the low-ELA phases coincide with, or are preceded by, high stratospheric sulfate loads from volcanic eruptions.

4 Discussion

Figure 1 shows the remarkable result that one single ELA history (Fig. 3) explains the long term GLCs of seven Alpine glaciers with very different geometries. This result justifies a posteriori the important assumption that all GLCs are caused by the same ELA history. Even if all glaciers are in the same mountain range and within 130 km of each other, local climate, and especially precipitation, vary on short spatial scales (e.g. Frei and Schär, 1998; Casty et al., 2005). Our assumption of similar ELA variation is supported by the observation that glacier mass balance variations, and hence ELA variations, are dominated by summer temperature and radiation (Ohmura et al., 1992; Vincent et al., 2004; Huss et al., 2009; Oerlemans, 2010; Thibert et al., 2013). Long-term instrumental records show that variations in these quantities are closely linked over the Alps (e.g. Casty et al., 2005; Auer et al., 2007; Huss et al., 2009).

Earlier climate reconstructions from GLCs (Klok and Oerlemans, 2003; Oerlemans, 2005; Leclercq et al., 2011; Leclercq and Oerlemans, 2012) used a linear response model to derive temperature for each glacier individually from smoothed length data. By contrast, the presented method uses a more accurate representation of macro-scopic glacier dynamics (LV-model, Eq. 1), unaltered and much longer GLC records, and optimizes on a single ELA history constrained by the responses of seven glaciers with very different geometries.

An important aspect of the presented method is that terminus positions documented for some glaciers can be used to infer missing data of the remaining glaciers. A sufficiently long calibration time span with well-documented glacier advances and retreats is a prerequisite to obtain good parameters for the DESM glacier models. Obviously, modeled GLCs still differ from reality by the dynamical effects of small scale terminus topography, but the overall timing and range of GLCs are stable.

4.1 Warm periods

The ELA values during warm periods with significant glacier retreat cannot be inferred from the terminus position record because of lack of data on minimum extents for the considered glaciers (which might still be buried under ice). Extended warm periods with glacier extents equal to, or smaller than today are possible within the gaps in the record, i.e. between 650–800, 850–950, 980–1050, 1200–1280, and 1400–1550 C.E. Recent findings of washed-out peat and wood from pro-glacial forefields of other Alpine glaciers indicate glacier extents smaller than present during the Holocene optimum climates between 690–780 (Hormes et al., 2001, 2006; Joerin et al., 2006). No similar findings are reported for the other periods.

4.2 Climatic interpretation

For the climatic interpretation of the reconstructed ELA history it is important to discern the different climate components. Summer mass balance, the balance component with high interannual variability, depends mainly (75 %) on temperature and to a lesser degree (25 %) on radiation (Ohmura et al., 2007) while winter mass balance is dominated by solid precipitation. The influence of precipitation on the ELA is relatively small: 1 K temperature change is equivalent to a precipitation change of $350\,\mathrm{mm\,yr^{-1}}$ w.e., or a radiation change of $7\,\mathrm{W\,m^{-2}}$ (Ohmura et al., 1992). The importance of atmospheric radiation variations (solar dimming through aereosols; changes in cloudiness) on mass balance has been highlighted by Huss et al. (2009). In a longer term context, summer temperature and precipitation have been identified as dominant controls on Aletsch glacier mass balance (Steiner et al., 2005, 2008).

4.2.1 Total solar irradiance

Several recent studies state that GLCs are closely related to total solar irradiance (TSI), although the similarity is only limited to several time spans (e.g. Beer et al., 2009;

Nussbaumer et al., 2011). Since GLCs are mostly a delayed reaction to climate forcing, a more direct relationship should exist between ELA variations and shortwave radiation. The comparison with TSI in Fig. 3b does not support the hypothesis of a direct influence of solar variability on glacier mass balance, except for the limited time span 1700–1950 where the similarity is striking. After 1950 the TSI is declining, whereas ELA is strongly rising. Before 1700 the two quantities seem mostly unrelated.

From the ELA sensitivity given in Table 2 a TSI change of $1\,\mathrm{W\,m^{-2}}$ would lead to an ELA increase of 200 m (fitted on the last 200 yr). This sensitivity is considerably higher than derived in the analysis by Ohmura et al. (1992) who find that a radiation change of $7\,\mathrm{W\,m^{-2}}$ is needed to compensate a 1 K temperature change, corresponding to a 100 m ELA change. An ELA sensitivity in this range would be achieved using the TSI scaling of Shapiro et al. (2011).

The above reasoning does not exclude the potentially important radiation modulation by atmospheric processes (aerosols, moisture, cloudiness) which is likely important for glacier mass balance (Ohmura et al., 2007; Huss et al., 2009). Since no long-term reconstructions of these parameters exist, their influence cannot be meaningfully investigated with the presented ELA reconstruction.

4.2.2 Volcanic cooling

A potentially important cause for the episodic and rapid glacier advances, reflected in the reconstructed low ELA periods, is radiative summer cooling big volcano eruptions. Stratospheric sulfate areosols from large explosive tropical volcano eruptions cause northern hemispheric summer cooling and altered circulation patterns (e.g. Crowley, 2000; Robock, 2000). They cause incoming solar radiation reduction by several $\mathrm{W\,m^{-2}}$ for two years, and decay on decadal time scale (e.g. Robock, 2000; Weber, 2005; Fischer et al., 2007). The direct effect of this cooling has been identified in tree ring widths (Breitenmoser et al., 2012) and latewood density, and an effect of 0.2 K cooling lasting about four years in Central Europe was inferred (Esper et al., 2013b). The full range of cold periods caused by volcanic events might not even be recorded (Mann

et al., 2012), but the hypothesis of missing years in the tree ring record was rejected (Esper et al., 2013a). Longer term persistence of cold summers is likely through sea ice/ocean feedback mechanisms, possibly even explaining the onset of the LIA cold period (Miller et al., 2012), although this is a topic under debate (Esper et al., 2013b).

Northern Hemisphere stratospheric sulfate loads reconstructed from ice core data (Gao et al., 2008) are shown in panels A of Figs. 2–4. It is striking that most reconstructed low-ELA phases coincide with, or are closely preceded by, high stratospheric sulfate loads (marked with gray vertical bars). Thus volcanic cooling explains most of the short-lived, rapid glacier advances during the LIA, which were recorded for the glaciers Bossons, Mer de Glace, and Unterer Grindelwald.

Before 1600 C.E. such a close correlation between volcanic activity and ELA respectively GLCs is not discernible. Whether this is due to the much sparser glacier length data, only recording large advances and thus leading to a less constrained ELA history, or to other causes cannot be assessed. Among the low-ELA phases without accompanying volcanic event, those of 510–580, 810–830, and 1330–1340 all correspond to cold phases in the temperature reconstructions from Büntgen et al. (2011) and PAGES 2k consortium (2013). These temperature records might already carry the imprint of volcanic cooling, but the direct effect on glacier mass balance through an altered energy balance is not visible in the record.

In view of the above close correspondence of volcanic eruptions with low reconstructed ELAs, and thus glacier advances, the absence of any recorded glacier advance after the very large 1258 volcanic eruption (Oppenheimer, 2003) is noteworthy. Although the dimming effect of volcanic aerosols only pertains for a few years, advances of several 100 m of the steep glaciers (Bossons, Mer de Glace, Rosenlaui) were recorded following each volcanic event after 1600. The lack of traces of a glacier advance after 1258 hints to small glacier extents during the period 1200–1300.

4.2.3 Atlantic Meridional Oscillation

Huss et al. (2010) concluded from a study of 20th century glacier mass balance that the Atlantic Meridional Oscillation (AMO) strongly influences glacier mass balance in the Alps. Figure 3c shows the comparison between a long AMO record (Mann et al., 2009) and the reconstructed ELA history. After 1250 C.E. the timing of warm and cold phases and the variability is very similar, although the low ELA events still would have to be explained by volcanic cooling. Our ELA reconstruction could thus be interpreted to support the hypothesis that the AMO influences mass balance of Alpine glaciers.

4.3 The riddle of the Little Ice Age glacier advance

Several studies concluded that the rapid glacier advances during the Little Ice Age (LIA, ca. 1550–1850 C.E.), and the last maximum extent around 1850–1865 cannot be explained using homogenized instrumental temperature data (e.g. Nesje and Dahl, 2003; Vincent et al., 2005; Lüthi et al., 2010; Nussbaumer et al., 2011). Likely processes leading to this rapid glacier growth are increased accumulation due to 25 % higher winter precipitation than present (Vincent et al., 2005), or reduced melt due to lower incoming short-wave radiation (Miller et al., 2012). More qualitatively, Nussbaumer et al. (2011) conclude that "a combination of low solar forcing, frequent and strong volcanic eruptions, and dynamic effects due to internal variability of the climate system led to the prominent glacier advances during the LIA". The rapid recession of the glaciers after 1865 has been explained by glacier surface darkening, and thus albedo reduction, by increasing release of industrial black carbon (Painter et al., 2013).

The agreement between our ELA reconstruction and several reconstructions of temperature (Fig. 4e, PAGES 2k consortium, 2013; f, Büntgen et al., 2006; g, Büntgen et al., 2011) and AMO index (Fig. 3c, Mann et al., 2009) show that additional large changes in winter precipitation are not needed to explain the rapid glacier advances, although higher summer precipitation has been found between 1700 and 1810 in tree ring reconstruction (Büntgen et al., 2011), and wetter winters were frequent between

1800–1850 (Pauling and Paeth, 2007). The frequent short phases of very low ELA during the LIA can be mostly explained by the effect of volcanic eruptions on incoming radiation. Also the rapid melt-back of the glaciers after 1860 can be explained by temperature alone, without additional albedo changes due to black carbon (Painter et al., 2013).

The question remains why before 1850 the homogenized instrumental temperature records (Casty et al., 2005; Auer et al., 2007) are considerably (~ 0.5–1 K) higher than the recent temperature reconstructions of Buentgen (tree rings) and PAGES (multi-proxy). One explanation is that early instrumental measurements were biased because of inadequate shading from solar radiation of the thermometers (Frank et al., 2007; Böhm et al., 2010). Another possible explanation is the lack of instrumental temperature data from the Alps before 1850 which requires the extrapolation of data from distant stations.

5 Conclusions

The presented method to reconstruct ELA variations from a set of GLC records yielded a new 1600 yr temperature reconstruction which is independent of other instrumental or proxy data. Through the simultaneous optimization on the GLCs of seven glaciers with one ELA history the result is less susceptible to geometry-dependent peculiarities of terminus dynamics of individual glaciers. Resulting GLCs automatically fill gaps in individual length change records, and recorded variability from fast-reacting glaciers are transferred to slowly-reacting glaciers.

The obtained ELA history agrees well with tree-ring derived and multi-proxy temperature reconstructions. Also a close correspondence with the AMO index between 1250–2010 could be observed. Long-term and short-term variability of these reconstructions are reproduced with the glacier record. This shows that analysis of temperature records with independent GLC records is a useful tool to independently validate these proxy-based reconstructions.

LIA climate from glacier fluctuations

M. P. Lüthi

Additionally, the reconstructed ELA history shows cold phases only partially recorded in the proxy records, most of which closely correspond to explosive tropical volcanic eruptions. This hints to a strong direct influence of stratospheric radiation scattering from volcanic aerosols on the energy balance on the glacier surface. The dependence of glacier mass balance on radiative forcing and the cooling due to changing stratospheric volcanic aerosols are not yet well understood.

The documented rapid advances of Alpine glaciers during the LIA, and their rapid retreat after 1865, can be reproduced with ELA changes that correspond to temperature reconstructions, additionally taking into account poorly quantified volcanic cooling from large eruptions. Alternative explanations stressing the importance of increased winter precipitation or increased ablation area albedo changes due to industrial black carbon, are not needed to explain the observations. Work to identify the relative importance of different proxies in the resulting GLCs with help of macroscopic glacier models is currently under way.

An additional avenue for further analysis are the glacier volume changes that the LV-model calculates simultaneously. After calibration with measured volume change data, such model results could be used to quantify long term runoff changes from glaciers. Such an analysis might decide a 150 yr old dispute whether glacier melt is to blame for frequent flooding and very high lake levels in the 1870–1880s, which was the main reason for the long and detailed investigation of glacier changes.

References

Auer, I., Böhm, R., Jurkovic, A., Lipa, W., Orlik, A., Potzmann, R., Schöner, W., Ungersböck, M., Matulla, C., Briffa, K., Jones, P., Efthymiadis, D., Brunetti, M., Nanni, T., Maugeri, M., Mercalli, L., Mestre, O., Moisselin, J.-M., Begert, M., Müller-Westermeier, G., Kveton, V., Bochnicek, O., Stastny, P., Lapin, M., Szalai, S., Szentimrey, T., Cegnar, T., Dolinar, M.,

Gajic-Capka, M., Zaninovic, K., Majstorovic, Z., and Nieplova, E.: HISTALP – historical instrumental climatological surface time series of the greater Alpine region 1760–2003, Int. J. Climatol., 27, 17–46, 2007. 5154, 5156, 5161, 5171, 5173

Beer, J., Abreu, J. A., and Steinhilber, F.: Sun and planets from a climate point of view, in: Universal Heliophysical Processes, no. 257 in Proceedings IAU Symposium, doi:10.1017/S1743921309029056, 2009. 5148, 5157

Begert, M., Schlegel, T., and Kirchhofer, W.: Homogeneous temperature and precipitation series of Switzerland from 1864 to 2000, Int. J. Climatol., 25, 65–80, 2005. 5154, 5171, 5173

Böhm, R., Jones, P., Hiebl, J., Frank, D., Brunetti, M., and Maugeri, M.: The early instrumental warm-bias: a solution for long central european temperature series 1760–2007, Climatic Change, 101, 4167, doi:10.1007/s10584-009-9649-4, 2010. 5154, 5161

Breitenmoser, P., Beer, J., Brönnimann, S., Frank, D., Steinhilber, F., and Wanner, H.: Solar and volcanic fingerprints in tree-ring chronologies over the past 2000 years, Palaeogeogr. Palaeocl., 313–314, 127–139, doi:10.1016/j.palaeo.2011.10.014, 2012. 5158

Büntgen, U., Frank, D. C., Nievergelt, D., and Esper, J.: Summer Temperature Variations in the European Alps, A.D. 755–2004, J. Climate, 19, 5606–5623, 2006. 5148, 5155, 5160, 5171, 5175

Büntgen, U., Tegel, W., Nicolussi, K., McCormick, M., Frank, D., Trouet, V., Kaplan, J. O., Herzig, F., Heussner, K.-U., Wanner, H., Luterbacher, J., and Esper, J.: 2500 years of European climate variability and human susceptibility, Science, 331, 578–582, doi:10.1126/science.1197175, 2011. 5148, 5155, 5159, 5160, 5171, 5175

Callendar, G.: Note on the relation between the height of the firn line and dimensions of a glacier, J. Glaciol., 1, 459–461, 1950. 5149

Casty, C., Wanner, H., Luterbacher, J., Esper, J., and Böhm, R.: Temperature and precipitation variability in the European Alps since 1500, Int. J. Climatol., 25, 1855–1880, doi:10.1002/joc.1216, 2005. 5154, 5156, 5161, 5171, 5173

Chen, J. and Funk, M.: Mass balance of Rhonegletscher during 1882/83–1986/87, J. Glaciol., 36, 199–209, 1990. 5152

Crowley, T.: Causes of climate change over the past 1000 years, Science, 289, 270–277, 2000. 5158

Esper, J., Büntgen, U., Luterbacher, J., and Krusic, P. J.: Testing the hypothesis of post-volcanic missing rings in temperature sensitive dendrochronological data, Dendrochronologia, 31, 216–222, doi:10.1016/j.dendro.2012.11.002, 2013a. 5159

Title Page

Abstract | Introduction

Conclusions | References

Tables | Figures

◄ | ►

◄ | ►

Back | Close

Full Screen / Esc

Printer-friendly Version

Interactive Discussion

Esper, J., Schneider, L., Krusic, P. J., Luterbacher, J., Büntgen, U., Timonen, M., Sirocko, F., and Zorita, E.: European summer temperature response to annually dated volcanic eruptions over the past nine centuries, Bull. Vocanol., 75, 736, doi:10.1007/s00445-013-0736-z, 2013b. 5158, 5159

Fischer, E. M., Luterbacher, J., Zorita, E., Tett, S. F. B., Casty, C., and Wanner, H.: European climate response to tropical volcanic eruptions over the last half millennium, Geophys. Res. Lett., 34, L05707, doi:10.1029/2006GL027992, 2007. 5158

Frank, D., Büntgen, U., Böhm, R., and Maurizio Maugeri, J. E.: Warmer early instrumental measurements vs. colder reconstructed temperatures: shooting at a moving target, Quaternary Sci. Rev., 26, 3298–3310, 2007. 5154, 5161

Frei, C. and Schär, C.: A precipitation climatology of the Alps from high-resolution rain-gauge observations, Int. J. Climatology, 18, 873–900, 1998. 5156

Gao, C., Robock, A., and Ammann, C.: Volcanic forcing of climate over the past 1500 years: an improved ice core-based index for climate models, J. Geophys. Res., 113, D23111, doi:10.1029/2008JD010239, 2008. 5155, 5159, 5173, 5174, 5175

Glaciological Reports: The Swiss Glaciers, 1880–2006/07, Tech. Rep. 1–128, Yearbooks of the Cryospheric Commission of the Swiss Academy of Sciences (SCNAT), published since 1964 by Laboratory of Hydraulics, Hydrology and Glaciology (VAW) of ETH Zürich, available at: http://glaciology.ethz.ch/swiss-glaciers/, 1881–2011. 5150

Greuell, W.: Hintereisferner, Austria: mass-balance reconstruction and numerical modelling of the historical length variations, J. Glaciol., 38, 233–244, 1992. 5149

Guiot, J., Corona, C., and ESCARSEL members: Growing season temperatures in Europe and climate forcings over the past 1400 years, PLOS One, 5, e9972, doi:10.1371/journal.pone.0009972.g001, 2010. 5148

Harrison, W. D., Raymond, C., Echelmeyer, K., and Krimmel, R.: A macroscopic approach to glacier dynamics, J. Glaciol., 49, 13–21, 2003. 5149

Hoelzle, M., Haeberli, W., Dischl, M., and Peschke, W.: Secular glacier mass balances derived from cumulative glacier length changes, Global Planet. Change, 36, 295–306, doi:10.1016/S0921-8181(02)00223-0, 2003. 5149

Holzhauser, H.: Zur Geschichte des Gornergletschers, Vol. G 84, Geographica Bernensia, 2011. 5170

Holzhauser, H. and Zumbühl, H.: Nacheiszeitliche Gletscherschwankungen, Tech. rep., Hydrologischer Atlas der Schweiz, Sonderdruck zum 54. Deutschen Geographentag, 2003. 5170

LIA climate from glacier fluctuations

M. P. Lüthi

Title Page

Abstract | Introduction

Conclusions | References

Tables | Figures

|◄ | ►|

◄ | ►

Back | Close

Full Screen / Esc

Printer-friendly Version

Interactive Discussion

Holzhauser, H., Magny, M., and Zumbühl, H.: Glacier and lake-level variations in west-central Europe over the last 3500 years, The Holocene, 15, 789–801, 2005. 5170

Hormes, A., Müller, B. U., and Schlüchter, C.: The Alps with little ice: evidence for eight Holocene phases of reduced glacier extent in the Central Swiss Alps, The Holocene, 11, 255–265, doi:10.1191/095968301675275728, 2001. 5157

Hormes, A., Beer, J., and Schlüchter, C.: A geochronological approach to understanding the role of solar activity on Holocene glacier length variability in the Swiss Alps, Geogr. Ann., 88, 281–294, doi:10.1111/j.0435-3676.2006.00301.x, 2006. 5157

Huss, M., Bauder, A., Funk, M., and Hock, R.: Determination of the seasonal mass balance of four Alpine glaciers since 1865, J. Geophys. Res., 113, F01015, doi:10.1029/2007JF000803, 2008. 5152, 5155

Huss, M., Funk, M., and Ohmura, A.: Strong Alpine glacier melt in the 1940s due to enhanced solar radiation, Geophys. Res. Lett., 36, L23501, doi:10.1029/2009GL040789, 2009. 5150, 5156, 5157, 5158

Huss, M., Hock, R., Bauder, A., and Funk, M.: 100-year glacier mass changes in the Swiss Alps linked to the Atlantic Multidecadal Oscillation, Geophys. Res. Lett., 36, L10501, doi:10.1029/2010GL042616, 2010. 5160

IPCC: Climate Change 2007, the Physical Scientific Basis, Contributions of Working Group I to the Fourth Assessment Report of the Intergovernmental Panel on Climate Change, Tech. rep., WMO/UNEP, Cambridge University Press, available at: http://www.ipcc.ch/publications_and_data/ar4/wg1/en/contents.html, 2007. 5148

Joerin, U. E., Stocker, T. F., and Schlüchter, C.: Multicentury glacier fluctuations in the Swiss Alps during the Holocene, The Holocene, 16, 697–704, doi:10.1191/0959683606hl964rp, 2006. 5157

Johnson, S. G.: The NLopt nonlinear-optimization package, available at: http://ab-initio.mit.edu/nlopt, 2012. 5152

Klok, E. and Oerlemans, J.: Deriving historical equilibrium-line altitudes from a glacier length record by linear inverse modelling, The Holocene, 13, 343–351, 2003. 5149, 5156

Leclercq, P. W. and Oerlemans, J.: Global and hemispheric temperature reconstruction from glacier length fluctuations, Clim. Dynam., 38, 1065–1079, doi:10.1007/s00382-011-1145-7, 2012. 5149, 5156

Title Page

Abstract | Introduction

Conclusions | References

Tables | Figures

◄ | ►

◄ | ►

Back | Close

Full Screen / Esc

Printer-friendly Version

Interactive Discussion

Leclercq, P. W., Oerlemans, J., and Cogley, J. G.: Estimating the glacier contribution to sea-level rise for the period 1800–2005, Surv. Geophys., 32, 519–535, doi:10.1007/s10712-011-9121-7, 2011. 5149, 5156

Leysinger-Vieli, G. J.-M. C. and Gudmundsson, G. H.: On estimating length fluctuations of glaciers caused by changes in climatic forcing, J. Geophys. Res., 109, f01007, doi:10.1029/2003JF000027, 2004. 5149

Lüthi, M. P.: Transient response of idealized glaciers to climate variations, J. Glaciol., 55, 918–930, 2009. 5149, 5151

Lüthi, M. and Bauder, A.: Analysis of Alpine glacier length change records with a macroscopic glacier model, Geogr. Helvetica, 65, 92–102, 2010. 5149

Lüthi, M. P., Bauder, A., and Funk, M.: Glacier volume change reconstruction from length change data of the Swiss Alps, J. Geophys. Res.-Earth, 115, F04022, doi:10.1029/2010JF001695, 2010. 5149, 5160

Mann, M. E., Zhang, Z., Rutherford, S., Bradley, R. S., Hughes, M. K., Shindell, D., Ammann, C., Faluvegi, G., and Ni, F.: Global signatures and dynamical origins of the Little Ice Age and Medieval Climate Anomaly, Science, 326, 1256–1260, doi:10.1126/science.1177303, 2009. 5148, 5155, 5160, 5171, 5174

Mann, M. E., Fuentes, J. D., and Rutherford, S.: Underestimation of volcanic cooling in tree-ring-based reconstructions of hemispheric temperatures, Nat. Geosci., 5, 202–205, doi:10.1038/NGEO1394, 2012. 5158

Messerli, B., Zumbühl, H. J., Amman, K., Kienholz, H., Oeschger, H., Pfister, C., and Zurbuchen, M.: Die Schwankungen des Unteren Grindelwaldgletschers seit dem Mittelalter, Zeitschrift für Gletscherkunde und Glazialgeologie, XI, 3–110, 1975. 5170

Miller, G. H., Geirsdóttir, À., Zhong, Y., Larsen, D. J., Otto-Bliesner, B. L., Holland, M. M., Bailey, D. A., Refsnider, K. A., Lehman, S. J., Southon, J. R., Anderson, C., Björnsson, H., and Thordarson, T.: Abrupt onset of the Little Ice Age triggered by volcanism and sustained by sea-ice/ocean feedbacks, Geophys. Res. Lett., 39, L02708, doi:10.1029/2011GL050168, 2012. 5159, 5160

Nesje, A. and Dahl, S. O.: The "Little Ice Age" – only temperature?, The Holocene, 13, 139–145, doi:10.1191/0959683603hl603fa, 2003. 5160

Nussbaumer, S. U. and Zumbühl, H. J.: The Little Ice Age history of the Glacier des Bossons (Mont Blanc massif, France): a new high-resolution glacier length curve based on historical documents, Climatic Change, 111, 301–334, doi:10.1007/s10584-011-0130-9, 2012. 5170

Title Page

Abstract | Introduction

Conclusions | References

Tables | Figures

◄ | ►

◄ | ►

Back | Close

Full Screen / Esc

Printer-friendly Version

Interactive Discussion

Nussbaumer, S., Zumbühl, H., and Steiner, D.: The history of the Mer de Glace AD 1570–2003 according to pictorial and written documents, Zeitschrift für Gletscherkunde und Glazialgeologie, 40, 2005. 5170

Nussbaumer, S. U., Steinhilber, F., Trachsel, M., Breitenmoser, P., Beer, J., Blass, A., Grosjean, M., Hafner, A., Holzhauser, H., Wanner, H., and Zumbühl, H. J.: Alpine climate during the Holocene: a comparison between records of glaciers, lake sediments and solar activity, J. Quaternary Sci., 26, 703–713, doi:10.1002/jqs.1495, 2011. 5148, 5158, 5160

Nye, J. F.: On the theory of the advance and retreat of glaciers, Geophys. J. Roy. Astr. S., 7, 431–456, 1963. 5149

Nye, J. F.: A numerical method of inferring the budget history of a glacier from its advance and retreat, J. Glaciol., 5, 589–607, 1965. 5149

Oerlemans, J.: Extracting a climate signal from 169 glacier records, Science, 308, 270–277, doi:10.1126/science.1107046, 2005. 5149, 5156

Oerlemans, J.: Estimating response times of Vadret da Morteratsch, Vadret da Palü, Briksdalsbreen and Nigardsbreen from their length records, J. Glaciol., 53, 357–362, 2007. 5149

Oerlemans, J.: The Microclimate of Valley Glaciers, Igitur, Utrecht Publishing & Archiving Services, iSBN 987-90-393-5305-5, 2010. 5154, 5156

Oerlemans, J.: Minimal Glacier Models, Igitur, Utrecht Publishing & Archiving Services, iSBN 978-90-6701-022-1, 2011. 5149

Ohmura, A., Kasser, P., and Funk, M.: Climate at the equilibrium line of glaciers, J. Glaciol., 38, 397–411, 1992. 5156, 5157, 5158

Ohmura, A., Bauder, A., Müller, H., and Kappenberger, G.: Long-term change of mass balance and the role of radiation, Ann. Glaciol., 46, 367–374, 2007. 5150, 5157, 5158

Oppenheimer, C.: Ice core and palaeoclimatic evidence for the timing and nature of the great mid-13th century volcanic eruption, Int. J. Climatol., 23, 417–426, doi:10.1002/joc.891, 2003. 5159

PAGES 2k consortium: Continental-scale temperature variability during the past two millennia, Nat. Geosci., 6, 339–346, doi:10.1038/NGEO1797, 2013. 5155, 5159, 5160, 5171, 5175

Painter, T. H., Flanner, M. G., Kaser, G., Marzeion, B., VanCuren, R. A., and Abdalati, W.: End of the Little Ice Age in the Alps forced by industrial black carbon, P. Natl. Acad. Sci. USA, doi:10.1073/pnas.1302570110, 2013. 5160, 5161

LIA climate from glacier fluctuations

M. P. Lüthi

Title Page

Abstract	Introduction
Conclusions	References
Tables	Figures

|◄ | ►|

◄ | ►

Back | Close

Full Screen / Esc

Printer-friendly Version

Interactive Discussion

Pauling, A. and Paeth, H.: On the variability of return periods of European winter precipitation extremes over the last three centuries, Clim. Past, 3, 65–76, doi:10.5194/cp-3-65-2007, 2007. 5161

Powell, M. J. D.: The BOBYQA algorithm for bound constrained optimization without derivatives, Tech. Rep. NA2009/06, Department of Applied Mathematics and Theoretical Physics, Cambridge, England, 2009. 5152

Robock, A.: Volcanic eruptions and climate, Rev. Geophys., 38, 191–219, doi:10.1029/1998RG000054, 2000. 5158

Roe, G. H. and O'Neal, M. A.: The response of glaciers to intrinsic climate variability: observations and models of late-Holocene variations in the Pacific Northwest, J. Glaciol., 55, 839–854, 2009. 5149

Schmeits, M. and Oerlemans, J.: Simulation of the historical variations in length of the Unterer Grindelwaldgletscher, J. Glaciol., 43, 152–164, 1997. 5149

Shapiro, A. I., Schmutz, W., Rozanov, E., Schoell, M., Haberreiter, M., Shapiro, A. V., and Nyeki, S.: A new approach to the long-term reconstruction of the solar irradiance leads to large historical solar forcing, Astron. Astrophys., 529, A67, doi:10.1051/0004-6361/201016173, 2011. 5158

Steiner, D., Walter, A., and Zumbühl, H.: The application of a non-linear back-propagation neural network to study the mass balance of Grosse Aletschgletscher, Switzerland, J. Glaciol., 51, 313–323, 2005. 5149, 5157

Steiner, D., Pauling, A., Nussbaumer, S. U., Nesje, A., Luterbacher, J., Wanner, H., and Zumbühl, H. J.: Sensitivity of European glaciers to precipitation and temperature – two case studies, Climatic Change, 90, 413–441, doi:10.1007/s10584-008-9393-1, 2008. 5157

Steinhilber, F., Beer, J., and Fröhlich, C.: Total solar irradiance during the Holocene, Geophys. Res. Lett., 36, L19704, doi:10.1029/2009GL040142, 2009. 5155, 5171, 5174

Thibert, E., Eckert, N., and Vincent, C.: Climatic drivers of seasonal glacier mass balances: an analysis of 6 decades at Glacier de Sarennes (French Alps), The Cryosphere, 7, 47–66, doi:10.5194/tc-7-47-2013, 2013. 5150, 5154, 5156

Vincent, C.: Influence of climate change over the 20th Century on four French glacier mass balances, J. Geophys. Res., 107, 4375, doi:10.1029/2001GL014592, 2002. 5154

Vincent, C., Kappenberger, G., Valla, F., Bauder, A., Funk, M., and Le Meur, E.: Ice ablation as evidence of climate change in the Alps over the 20th century, J. Geophys. Res., 109, D10104, doi:10.1029/2003JD003857, 2004. 5150, 5156

Vincent, C., Le Meur, E., Six, D., and Funk, M.: Solving the paradox of the end of the Little Ice Age in the Alps, Geophys. Res. Lett., 32, L09706, doi:10.1029/2005GL022552, 2005. 5150, 5160

Weber, S. L.: A timescale analysis of the Northern Hemisphere temperature response to volcanic and solar forcing, Clim. Past, 1, 9–17, doi:10.5194/cp-1-9-2005, 2005. 5158

Zumbühl, H.: Die Schwankungen der Grindelwaldgletscher in den historischen Bild- und Schriftquellen des 12. bis 19. Jahrhunderts, Denkschriften der Schweizerischen Naturforschenden Gesellschaft, 92, 279, 1980. 5170

Zumbühl, H. and Holzhauser, H.: Alpengletscher in der Kleinen Eiszeit, Die Alpen, Sonderheft zum 125.-jährigen Jubiläum des SAC, 64, 130–322, 1988. 5153, 5170

Title Page

Abstract | Introduction

Conclusions | References

Tables | Figures

◄ | ►

◄ | ►

Back | Close

Full Screen / Esc

Printer-friendly Version

Interactive Discussion

Table 1. Sources of glacier length change data used in this study.

Glacier	Time span	Source
Bossons	1580–2010	Nussbaumer and Zumbühl (2012)
Gorner	450–2010	Zumbühl and Holzhauser (1988); Holzhauser (2011)
Grosser Aletsch	67–2010	Holzhauser et al. (2005)
Mer de Glace	1575–2010	Nussbaumer et al. (2005)
Rhone	1602–2010	Zumbühl and Holzhauser (1988)
Rosenlaui	1760–2010	Zumbühl and Holzhauser (1988)
Unterer Grindelwald	393–1983	Messerli et al. (1975); Zumbühl (1980)
		Holzhauser and Zumbühl (2003)

Table 2. ELA sensitivity factors f_s used in the data comparisons in Figs. 2–4.

Var	Data source	Type	f_s
T	Gd. S. Bernard (Begert et al., 2005)	instr.	$100\,\mathrm{m\,K^{-1}}$
T	HISTALP (Auer et al., 2007)	instr.	$100\,\mathrm{m\,K^{-1}}$
T	Casty et al. (2005)	instr.	$100\,\mathrm{m\,K^{-1}}$
T	Büntgen et al. (2006)	dendro	$70\,\mathrm{m\,K^{-1}}$
T	Büntgen et al. (2011)	dendro	$70\,\mathrm{m\,K^{-1}}$
T	PAGES 2k consortium (2013)	multi	$120\,\mathrm{m\,K^{-1}}$
T	Mann et al. (2009)	multi	$200\,\mathrm{m\,K^{-1}}$
AMO	Mann et al. (2009)	multi	$200\,\mathrm{m\,K^{-1}}$
TSI	Steinhilber et al. (2009)	solar	$200\,\mathrm{W\,m^{-2}}$
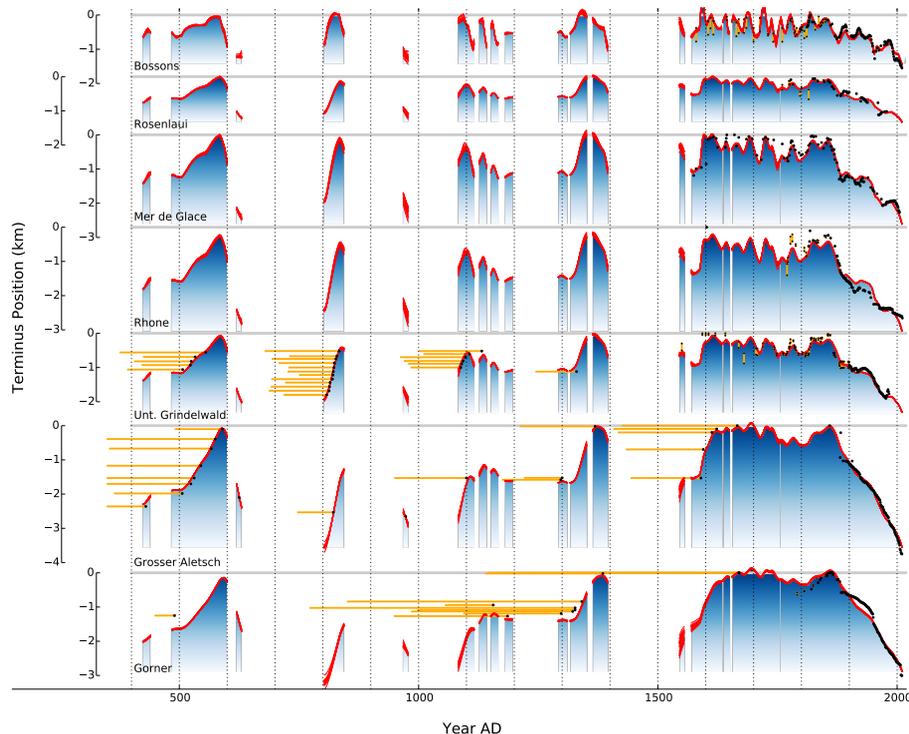
Fig. 1. Comparison of modeled and measured terminus position histories of seven glaciers. Results from the 20 best-matching model runs are shown with red lines. No model results are shown in intervals without length constraints. Black dots mark individual terminus position measurements, orange horizontal lines the life spans of trees killed by advancing glaciers (Table 1 for data sources).
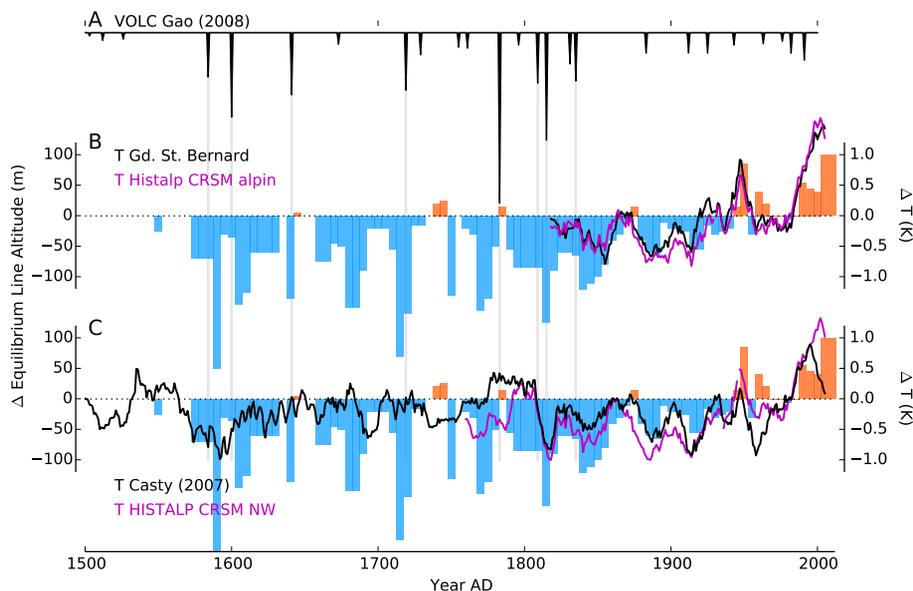
Fig. 2. ELA variation reconstruction leading to best agreement with length change records from seven glaciers (Fig. 1). Modeled ELAs are shown with red and blue colored areas. Instrumental records are shown for comparison in panels **(B)** and **(C)** as 11 yr running means. Data sets are from MeteoSwiss (Begert et al., 2005), Casty et al. (2005) and HISTALP (Auer et al., 2007). **(A)** and vertical stripes show timing and magnitude of Northern Hemisphere stratospheric sulfate loading from explosive volcanism (Gao et al., 2008).

Title Page

Abstract | Introduction

Conclusions | References

Tables | Figures

|◀ | ▶|

◀ | ▶

Back | Close

Full Screen / Esc

Printer-friendly Version

Interactive Discussion

Full Screen / Esc

Printer-friendly Version

Interactive Discussion
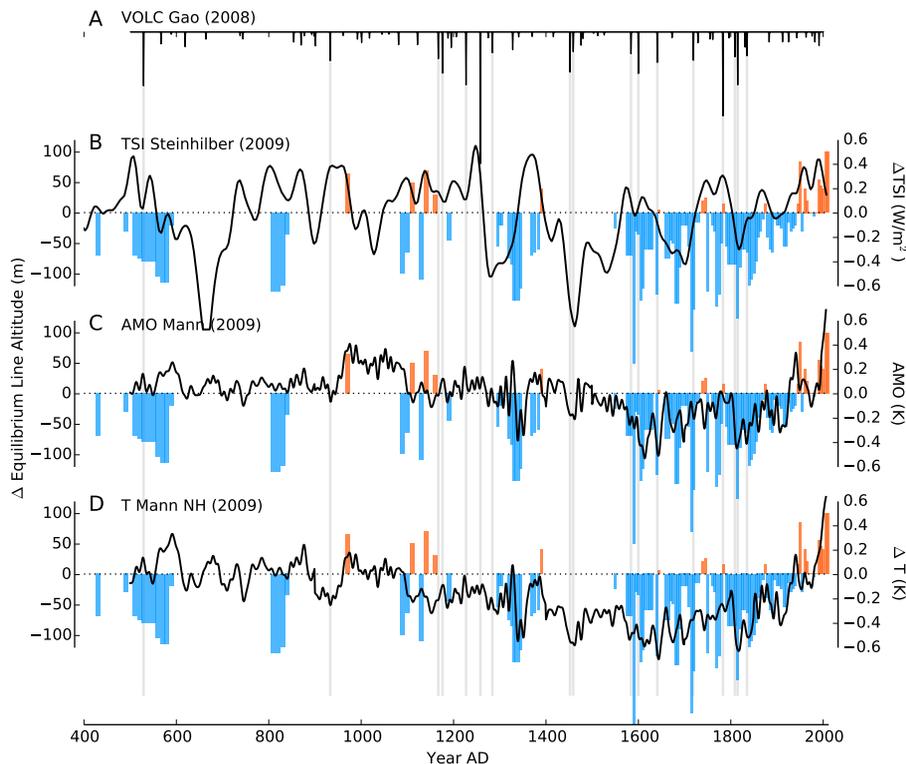
Fig. 3. ELA variation reconstruction for the time span 400–2010 compared to climate records from different proxies. **(A)** Northern Hemisphere stratospheric sulfate loading from explosive volcanism (Gao et al., 2008). **(B)** total solar irradiance (TSI, red; Steinhilber et al., 2009), **(C)** AMO index reconstruction (black; Mann et al., 2009), **(D)** multi-proxy temperature reconstruction (Mann et al., 2009).
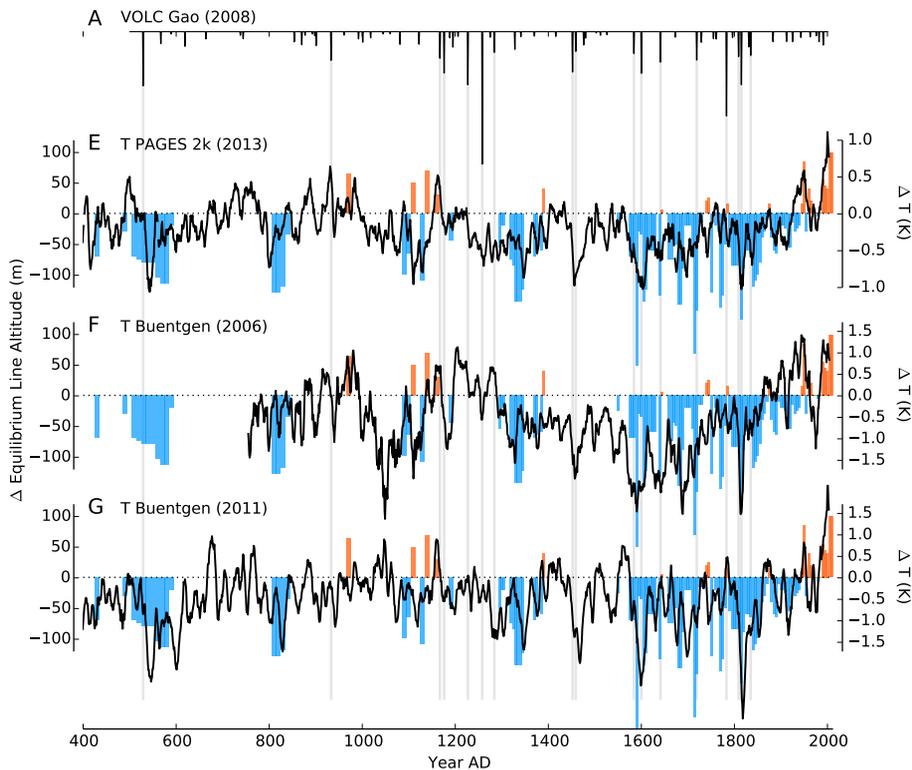
Fig. 4. ELA variation reconstruction for the time span 400–2010 compared to climate records from different proxies. **(A)** Northern Hemisphere stratospheric sulfate loading from explosive volcanism (Gao et al., 2008). **(E)** multi-proxy temperature reconstruction (PAGES 2k consortium, 2013). **(F, G)** temperature reconstructions from tree rings (Büntgen et al., 2006, 2011). All temperature curves are smoothed with a 7 yr running mean.